

RESEARCH

Open Access



A novel IgG-Fc-Fused multiepitope vaccine against *Brucella*: robust immunogenicity

Aodi Wu^{1†}, Yuting Zhang^{1†}, Caidong Liu³, Kaiat Zhumanov⁴, Tao He¹, Kexin Yan¹, Honghuan Li¹, Shuangshaung Fu¹, Xin Li¹, Wenxiang Zhang¹, Chuang Meng⁵, Changsuo Zhang⁶, Jinliang Sheng¹, Zhongchen Ma¹, Mingguo Xu¹, Junbo Zhang^{2*}, Jihai Yi^{1*} and Yueli Wang^{3*}

Abstract

Brucellosis is one of the most common zoonotic diseases caused by *Brucella* spp. However, there is currently no *Brucella* vaccine available for humans. Although some attenuated live vaccines have been approved for animals, their protective efficacy is suboptimal. In previous studies, we utilized an epitope- and structure-based vaccinology platform to identify the immunodominant epitopes of *Brucella* antigens OMP19, OMP16, OMP25, and L7/L12, and constructed the multi-epitope vaccine MEV-Fc against *Brucella*. In this study, OMP19, OMP16, OMP25, and L7/L12, and MEV-Fc was expressed and purified via an *Escherichia coli* expression system, which validated that MEV-Fc possesses high immunological efficacy and exerts a significant protective effect in BALB/c mice within the *Brucella* infection model. MEV-Fc enhanced Th1 and Th2 immune responses and strongly induced the production of the pro-inflammatory cytokine IFN- γ . Furthermore, MEV-Fc protected mice against *Brucella* infection compared to control group (PBS). In conclusion, our results provide new insights and data support for the development of human *Brucella* vaccines.

Keywords *Brucella*, Multiple epitopes, Vaccines immune response

Introduction

Brucellosis is one of the most common zoonotic diseases worldwide, capable of being transmitting from animals to humans, causing severe infections in both animals and humans and affecting multiple body systems [1]. The high incidence rates in humans and animals render this infection a significant public health concern in underdeveloped countries, while also imposing considerable economic losses on animal production [2]. In livestock, this condition leads to abortion, stillbirth, infertility, higher mortality rates in young animals, prolonged calving intervals, reduced feed efficiency, weight loss, and decreased milk production [3]. Humans can contract the disease through direct contact with infected animals or consumption of contaminated raw dairy products [4]. Symptoms of human infection include fatigue, sweating, chills, fluctuating fever, myalgia, and arthralgia [5]. Currently,

[†]Aodi Wu and Yuting Zhang contributed equally to this work.

*Correspondence:

Junbo Zhang

zhangjunbo666@126.com

Jihai Yi

724050645@qq.com

Yueli Wang

577674101@qq.com

¹College of Animal Science and Technology, Shihezi University, Shihezi 832003, Xinjiang, China

²Guizhou Provincial Key Laboratory for Biodiversity Conservation and Utilization in the Fanjing Mountain Region, Tongren University, Tongren, Guizhou 554300, China

³School of Medicine, Shihezi University, Shihezi 832003, Xinjiang, China

⁴Kazakh National Agrarian University, 050010 Almaty, Kazakhstan

⁵Jiangsu Key Laboratory of Zoonosis, Yangzhou University, Yangzhou, China

⁶Tiankang Biopharmaceutical Co., Ltd, 830032 Urumqi, Xinjiang, China



© The Author(s) 2025. **Open Access** This article is licensed under a Creative Commons Attribution-NonCommercial-NoDerivatives 4.0 International License, which permits any non-commercial use, sharing, distribution and reproduction in any medium or format, as long as you give appropriate credit to the original author(s) and the source, provide a link to the Creative Commons licence, and indicate if you modified the licensed material. You do not have permission under this licence to share adapted material derived from this article or parts of it. The images or other third party material in this article are included in the article's Creative Commons licence, unless indicated otherwise in a credit line to the material. If material is not included in the article's Creative Commons licence and your intended use is not permitted by statutory regulation or exceeds the permitted use, you will need to obtain permission directly from the copyright holder. To view a copy of this licence, visit <http://creativecommons.org/licenses/by-nc-nd/4.0/>.

vaccination stands as the most effective method for the prevention and control of this zoonotic disease. Live attenuated vaccines for veterinary use have been widely employed and play a critical role in controlling *brucellosis* epidemics; However, these live attenuated veterinary vaccines have several drawbacks, including human infection, spontaneous abortion in animals, antibiotic resistance, and insufficient protective efficacy [6, 7]. Currently, there is no approved vaccine for human infection caused by this pathogen. To safeguard the livelihood and health of populations at risk, especially slaughterhouse workers who face continuous exposure to infected animals, an urgent need exists to develop safe and effective alternatives to the existing live attenuated vaccines against this zoonotic disease.

Studies have shown that subunit vaccines exhibit high safety and specificity, with fewer side effects following vaccination [8]. However, due to limited antigenic epitopes, their protective efficacy is lower compared to traditional vaccines [9]. Over the past few decades, a variety of antigens, such as OMP19, OMP25, L7/L12, and OMP16, have been studied from *Brucella* [10–13]. They are considered promising candidate proteins due to their high immunogenicity and ability to induce in vivo immune protection. OMP16 and OMP19 are outer membrane lipoproteins located on the surface of *Brucella*, both exposed to the bacterial surface and commonly present across all *Brucella* strains. OMP25, a *Brucella* outer membrane protein, plays a critical role in maintaining membrane integrity due to its high conservation [14, 15]. *Brucella* ribosomal protein L7/L12, a conserved protein with immunogenic properties, plays an auxiliary role in immune protection. These antigens have demonstrated the ability to prevent *Brucella* infections by reducing bacterial loads in organs of mice. However, subunit vaccines using known antigens cannot achieve the protection levels conferred by live attenuated vaccines. Further studies are required to identify novel antigens to enhance vaccine efficacy [16]. Multiepitope vaccines have emerged as an attractive alternative to traditional live attenuated and inactivated vaccines due to their favorable safety profiles and ability to elicit targeted immune responses against specific epitopes [17].

Bioinformatics techniques have shown significant advantages in modern vaccine design and development, including ease of operation, cost efficiency, and higher success rates [18, 19]. Using this technology allows for efficient evaluation of the immunogenicity of candidate subunit vaccines. Particularly in multiepitope vaccine design, bioinformatics employs reliable in silico tools to predict MHC binding sites, T cell, and B cell epitopes, thereby significantly shortening development timelines and reducing risk and cost [20]. Compared to traditional laboratory methods, bioinformatics not only enhances

prediction accuracy but also facilitates the design of more effective vaccines tailored for the protection of various common hosts against different *Brucella* species [17, 21].

In this study, an epitope- and structure-based vaccinology platform was applied to develop a multiepitope candidate vaccine, MEV-Fc, composed of CTL, HTL, and B cell epitopes from OMP16, OMP19, L7/L12, and OMP25, along with molecular adjuvants and an Fc fragment. The antigenicity, physicochemical, and structural properties of the candidate vaccine were analyzed, and the rOMP16, rOMP19, rL7/L12, rOMP25, and rMEV-Fc proteins from *Brucella* were expressed and purified. Subsequently, their immunogenicity and protective efficacy were evaluated and compared in a *brucellosis* model using BALB/c mice.

Materials and methods

Animals and ethics statement

All animal experiments were approved by the Bioethics Committee of Shihezi University and conducted in accordance with the Committee's recommendations (A2024-436). The animal breeding was carried out at the Experimental Animal Center of the College of Animal Science and Technology, Shihezi University. The environmental temperature was controlled at $(23 \pm 3)^{\circ}\text{C}$ and the humidity at $(55\% \pm 5\%)$. Before use, materials such as cages, water bottles, and bedding were sterilized. Food, bedding, and water were replaced every four days.

Acquisition and construction of candidate vaccine sequences

The amino acid sequences of *Brucella* major antigens OMP19 (AAB06277.1), OMP16 (AEF59023.1), OMP25 (AFJ79953.1) and L7/L12 (AAL51929.1) were obtained from the NCBI database. Based on our previous research [22], the dominant CTL and HTL epitopes and B-cell epitopes of the antigens OMP16, OMP19, L7/L12, and OMP25 from *Brucella* were linked using GP/GPG linkers to form Multi-epitope Vaccines (MEV). The human beta-defensin 3 (hBD-3) sequence and a pan HLA-DR-binding epitope (PADRE) sequence were linked to the N-terminal of the MEV through EAAAK linkers. Moreover, the mouse IgG Fc fragment (P01868-1) sequence was linked to the C-terminal of the MEV via KK linkers, resulting in the complete vaccine construct sequence, named MEV-Fc. Finally, the DNA sequences for OMP16, OMP19, L7/L12, OMP25, and MEV-Fc were obtained through reverse translation and codon optimization of their amino acid sequences (Supplementary Table 1).

Evaluation of physicochemical properties of candidate vaccines

The characteristics of the candidate vaccine were evaluated using bioinformatics analysis software. First, the ProtParam server (<https://www.expasy.org/resources/pro>

tparam) was used to analyze its physicochemical properties [23]. Antigenicity and immunogenicity analyses were conducted using the VaxiJen v2.0 server [24] and the IEDB Class I Immunogenicity server [25]. Toxicity was assessed using ToxinPred, with the threshold value set at 0.6 [26].

Secondary and tertiary structure prediction

The secondary structure of MEV-Fc was predicted using the SOPMA secondary structure prediction tool (http://npsa-pbil.ibcp.fr/cgi-bin/npsa_automat.pl?page=/NPSA/npsa_sopma.html) [27]. The tertiary structure of MEV-Fc was predicted using the Robetta server (<http://rosetta.bakerlab.org/>) and further assessed through Swiss-model Structure Assessment and Ramachandran Plot (<https://www.wisemodel.expasy.org/assess>). The quality of the constructed model was evaluated. The Prosa web server (<https://prosa.services.came.sbg.ac.at/prosa.php/>) was used to further assess uncertainties in the tertiary structure [28].

Expression purification of recombinant proteins

After optimizing the synthesis of DNA sequences for OMP19, OMP16, L7/L12, OMP25, and MEV-Fc (Generalbiol, China), the sequences were inserted into the expression vector pET-22b (Ampicillin) and then transfected into *Escherichia coli* (BL21, DE3). Induction was performed overnight at 15 °C using 0.2 mM IPTG. The products were purified using high-affinity Ni-NTA resin (ClonTech, China). The concentration of the purified recombinant proteins was determined using a BCA protein assay kit (Thermo). Additionally, the proteins were analyzed using SDS-PAGE and western blot. Immunoblotting was performed with mouse monoclonal anti-His tag antibodies (Abcam, China) and goat anti-mouse IgG-HRP (H + L) antibodies (Abcam, China).

Animal immunization experiments

Sixty-three 6-week-old SPF BALB/c mice were randomly divided into seven groups: rOMP16 immunization group, rOMP19 immunization group, rL7/L12 immunization group, rOMP25 immunization group, rMEV-Fc immunization group, commercial attenuated strain S2 group, and PBS control group, with 9 mice in each group. The rMEV-Fc group ($n=9$) was subcutaneously injected with a mixture of recombinant protein and incomplete Freund's adjuvant (IFA, Sigma-Aldrich, Missouri, USA), while the control group ($n=9$) was subcutaneously injected with PBS. The concentration of the vaccine protein solution was 500 µg/mL. Each mouse received an injection of 100 µL, and the injections were administered every 2 weeks for a total of 2 doses. Seven weeks after immunization, spleen cells from the immunization groups and control groups were aseptically collected for experimental analysis.

Detection of IFN-γ secretion levels in mouse spleen lymphocytes by elispot

Spleen cells from immunized mice (42 d post-immunization) were aseptically isolated and collected according to the manufacturer's instructions (Tianjin Haoyang Biological Co., Ltd.). Heat-inactivated *B. melitensis* virulent strain M28 (HI M28) was used to stimulate spleen lymphocytes as per the manufacturer's protocol (Mabtech, Sweden), and T cells secreting IFN-γ in immunized mice were detected using the enzyme-linked immunospot assay (ELISpotBasic) kit.

Lymphocyte proliferation assay

Lymphocytes were extracted from mouse spleens using a lymphocyte isolation kit (Tbdscience, China). rOMP16, rOMP19, rL7/L12, rOMP25, rMEV-Fc proteins, or Concanavalin A (ConA) were used to stimulate lymphocytes. Then, CCK-8 reagent (Solarbio, China) was added according to the manufacturer's recommendations and incubated for 2 h. Absorbance was measured at OD_{450nm}. Absorbance was measured at OD_{450nm}. The stimulation index (SI) was calculated using the formula: (OD_{450nm} of protein-stimulated group - OD_{450nm} of blank group) / (OD_{450nm} of negative control group - OD_{450nm} of blank group).

Flow cytometry analysis of spleen lymphocytes in immunized mice

Forty-two days post-immunization, spleen lymphocytes were isolated and the cell suspensions were stained with FITC-conjugated anti-mouse CD4 (BioLegend, USA) and PE-conjugated anti-mouse CD8 (BioLegend, USA). The proportion of CD4⁺ and CD8⁺ T cells in spleen lymphocytes upon antigen re-encounter was analyzed.

Antibody determination by indirect enzyme-linked immunosorbent assay (iELISA)

The purified rOMP19, rOMP16, rOMP25, rL7/L12, and rMEV-Fc were diluted with carbonate buffer at pH 9.6 to a concentration of 1 µg/mL and then coated onto 96-well immunoassay plates at 100 µL per well. After blocking with 5% skim milk, the plates were incubated with appropriately diluted serum (1:1000) at 37 °C, followed by incubation with 1:50,000 diluted HRP-conjugated goat anti-mouse IgG, IgG1, or IgG2a antibodies (Abcam, China) at 37 °C. Color development was initiated with a one-component TMB substrate solution (CWBio, China), stopped using 50 µL stop solution (50 mM H₂SO₄), and optical density was measured at 450 nm using a microplate reader (Molecular Devices Corporation, CA, USA).

Measurement of cytokines in serum

Forty-two days post-immunization, mouse serum was collected and cytokines IFN- γ and IL-4 in serum were measured using commercial ELISA kits (R&D, USA).

Challenge of mice and determination of spleen bacterial load after infection

On the 49th day following the initial immunization, the mice were intraperitoneally challenged with 100 μ L of *B. melitensis* M28 (containing 5×10^5 CFU). Seven days later, the mice were euthanized via cervical dislocation and dissected under sterile conditions. The spleens were harvested, and homogenates were prepared using PBS. Spleen tissue homogenate (100 μ L) was spread onto *Brucella* solid medium (TSA) and cultured at 37 $^{\circ}$ C for 3 to 5 days. Colony counts were performed to calculate the bacterial load in the spleens of mice.

Safety determination

Six-week-old female BALB/c mice free of specific pathogens were divided into two groups ($n = 3$). One group of mice was injected with 100 μ g of rMEV-Fc per mouse, while the other group remained untreated. The body temperature and weight of the mice were measured on days 0, 1, 2, 5, 7, 10, 12, and 14 post-injection. On day 14 post-injection, mice were euthanized by cervical dislocation, and the hearts, livers, spleens, lungs, and kidneys were collected and fixed with 4% paraformaldehyde (Solarbio, China). The tissues were embedded, sectioned, dried in an oven, dewaxed, and rehydrated. Subsequently, the sections were stained, dehydrated, cleared for transparency, and sealed with neutral resin following the manufacturer’s instructions for the hematoxylin and eosin (HE) staining kit (Solarbio). On day 28 post-injection, blood was collected from the tail vein, and the levels of serum alanine aminotransferase (AST), alkaline phosphatase (ALP), blood urea nitrogen (BUN), and creatinine (CRE) were measured using the Chemray 240 automatic biochemical analyzer.

Statistical analysis

Statistical analysis was performed using GraphPad Prism version 9.5.0 (GraphPad, USA). Data were analyzed by one-way analysis of variance (ANOVA) with Dunn’s multiple comparison test. All data are presented as mean \pm standard deviation (SD). A p -value of

less than 0.05 was considered statistically significant (**** $p < 0.0001$, *** $p < 0.001$, ** $p < 0.01$, and * $p < 0.05$).

Results

Evaluation of physicochemical properties and prediction of secondary and tertiary structures of candidate vaccines

The physicochemical properties of vaccines significantly affect their immune functions [29]. Therefore, various physical and chemical properties of candidate vaccines were analyzed using ExPASy ProtParam server, VaxiJen v2.0 server, IEDB Class I Immunogenicity server, and ToxinPred server, as shown in Table 1. The results demonstrated that the candidate vaccines exhibited good stability, antigenicity, and immunogenicity, and were non-toxic, indicating their potential as suitable vaccine candidates.

In the results of secondary structure prediction, OMP19 has 14.69% Alpha helix, 18.64% Extended strand, and 66.67% Random coil; OMP16 has 44.05% Alpha helix, 12.50% Extended strand, and 43.45% Random coil; OMP25 has 19.57% Alpha helix, 20.87% Extended strand, and 59.57% Random coil; L7/L12 has 69.35% Alpha helix, 6.45% Extended strand, and 24.19% Random coil; MEV-Fc has 15.33% Alpha helix, 19.17% Extended strand, 7.17% Beta turn, and 58.33% Random coil.

We predicted the tertiary structures of candidate vaccines using the Robetta server and visualized them with PyMOL software (Fig. 1). To assess the quality of the models, we generated a Ramachandran plot for the predicted models using Swiss-Model Structure Assessment to evaluate the overall structural quality. The results showed that the percentages of OMP16, OMP19, L7/L12, OMP25, and MEV-Fc in the Ramachandran Favoured regions were 99.40%, 95.43%, 99.18%, 97.37%, and 94.31%, respectively (Supplementary Fig. 1). The Z-scores of the models for OMP16, OMP19, L7/L12, OMP25, and MEV-Fc were 5.02, 5.07, 4.92, 5.1, and 7.88, respectively, falling within the score range of natural proteins of similar sizes (Supplementary Fig. 2).

Expression, purification, and confirmation of recombinant proteins

We inserted the codon-optimized sequences of OMP16, OMP19, L7/L12, OMP25, and MEV-Fc into pET-22b (+). Subsequently, recombinant proteins were expressed using IPTG and purified through Ni-NTA agarose

Table 1 Predicted physicochemical properties of candidate vaccines

Protein name	Molecular weight (kDa)	Theoretical pI	Instability index	Aliphatic index	GRAVY	Vaxijenscore	Antigenicity
OMP16	18.2	9.92	43.86	78.57	-0.351	0.5500	ANTIGEN
OMP19	17.6	8.91	44.8	77.29	-0.1	0.6547	ANTIGEN
OMP25	24.7	9.28	13.81	73.48	-0.255	0.7575	ANTIGEN
L7/L12	12.5	4.79	18.55	108.87	0.119	0.5381	ANTIGEN
MEV-Fc	61.2	8.89	24.06	57.35	-0.5	1.0342	ANTIGEN

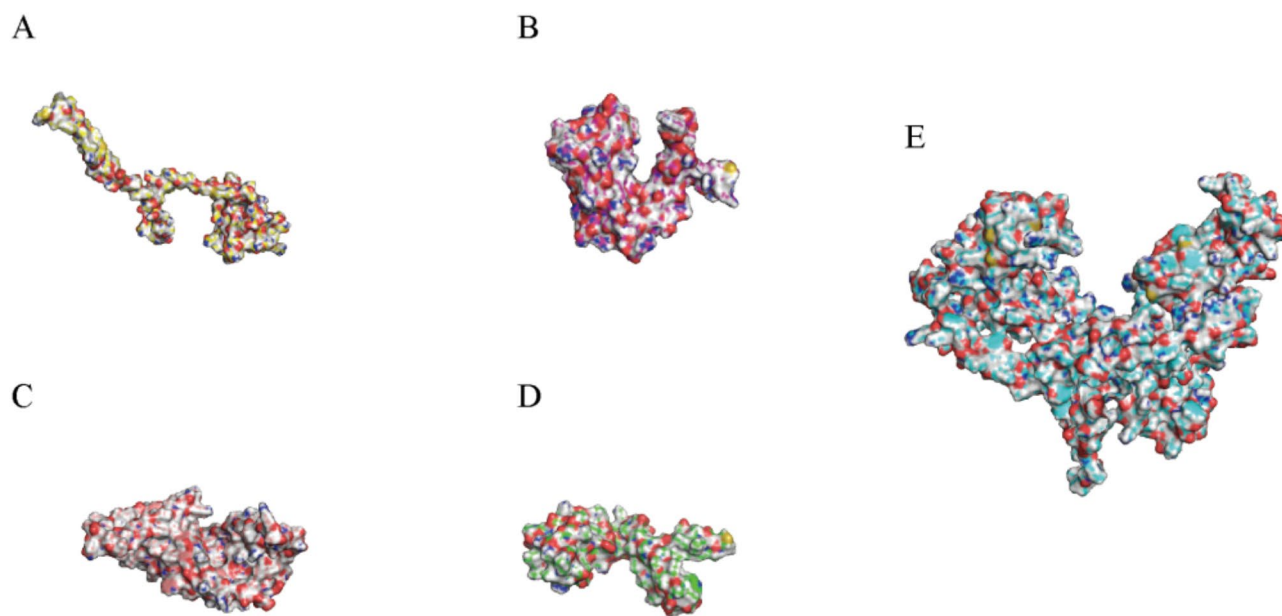


Fig. 1 Predicted Tertiary Structure of Candidate Vaccines. The three-dimensional models of OMP19 (A), OMP16 (B), OMP25 (C), L7/L12 (D), and MEV-Fc (E) were obtained from Robetta servers

(Qiagen) chromatography. Observable bands corresponding to the recombinant proteins were detected by SDS-PAGE (Fig. 2A). The expression of recombinant proteins was further validated using an anti-His tag antibody (Fig. 2B) and the sera from naturally infected *Brucella* cases (Supplementary Fig. 3).

Candidate vaccines induce specific antibodies and cytokine secretion in mice

We conducted a series of mouse experiments to further evaluate the immunogenicity of the candidate vaccines. BALB/c mice were subcutaneously injected with rOMP16, rOMP19, rL7/L12, rOMP25, and rMEV-Fc at days 0 and 14 (50 μ g per doses), and their effects on immune responses were observed and compared. On days 0, 7, 14, 21, 28, 35, 42, and 49, blood samples were collected from the tail veins of each mouse. PBS was used as the control (Fig. 3A). These samples were used to detect specific serum antibodies against OMP16, OMP19, L7/L12, OMP25, and MEV-Fc. iELISA results demonstrated that the IgG antibody levels in mouse serum increased rapidly 14 days after the primary immunization, reaching a peak at day 28 and persisting until day 49, compared to the control group, the total IgG levels in the immunized group showed statistically significant differences; no antibodies were detected in the control group (Fig. 3B), indicating that the candidate vaccines stimulated the production of high levels of specific antibodies. In addition, compared with the PBS group, the rMEV-Fc group induced high levels of IgG2a and IgG1 (Supplementary Fig. 4). Considering that the IgG2a/IgG1 ratio is often used as an indicator of potential Th1

or Th2 responses, we further calculated the ratios of different IgG subtypes and found that rMEV-Fc induced a mixed and balanced IgG2a/IgG1 systemic response (IgG2a/IgG1 ratio approximately 1.0) [30], suggesting that both Th1 and Th2 responses have been activated. On the other hand, rOMP16, rOMP19, and rL7/L12 favored Th1-type immune responses, while rOMP25 favored Th2-type responses [31, 32] (Fig. 3C). Moreover, The levels of the Th1 cytokine IFN- γ and the Th2 cytokine IL-4 in mouse serum 49 days post-immunization were determined using the ELISA method. The ELISA results revealed that the levels of IFN- γ in the rL7/L12 group, MEV-Fc group, and S2 group were significantly higher than those in the PBS control group (Fig. 3D). Compared to the PBS control group, the rMEV-Fc group showed a significant increase in IL-4 levels, while the other groups did not significantly differ from the control group (Fig. 3E). These findings indicate that rMEV-Fc is capable of effectively inducing the differentiation and proliferation of antigen-specific T cells.

The secretion of IFN- γ by splenic lymphocytes and the promotion of their proliferation induced by candidate vaccines

Spleen lymphocytes were isolated from mice 42 days post-immunization, and ELISpot was used to measure the numbers of antigen-stimulated specific T cells producing IFN- γ , an important indicator for evaluating vaccine-induced cellular immunity. The results showed that the numbers of IFN- γ -secreting T cells in the rOMP16 group, rMEV-Fc group, S2 group, and rOMP25 group were higher than those in the control group (PBS).

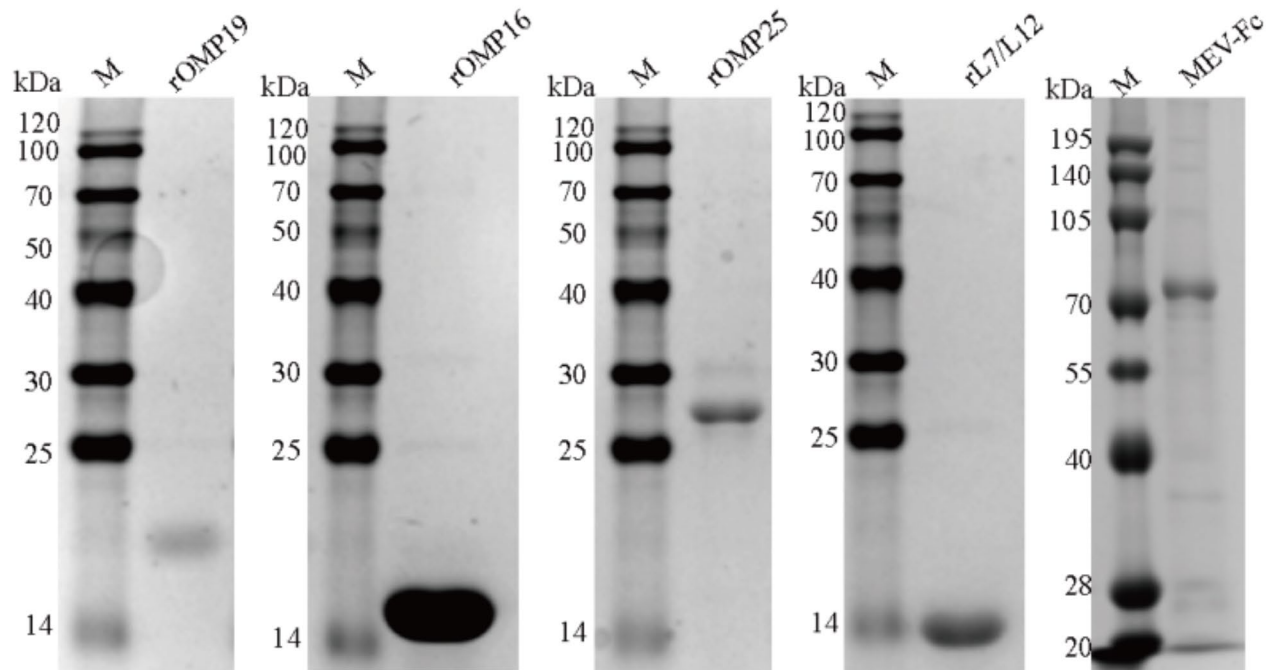
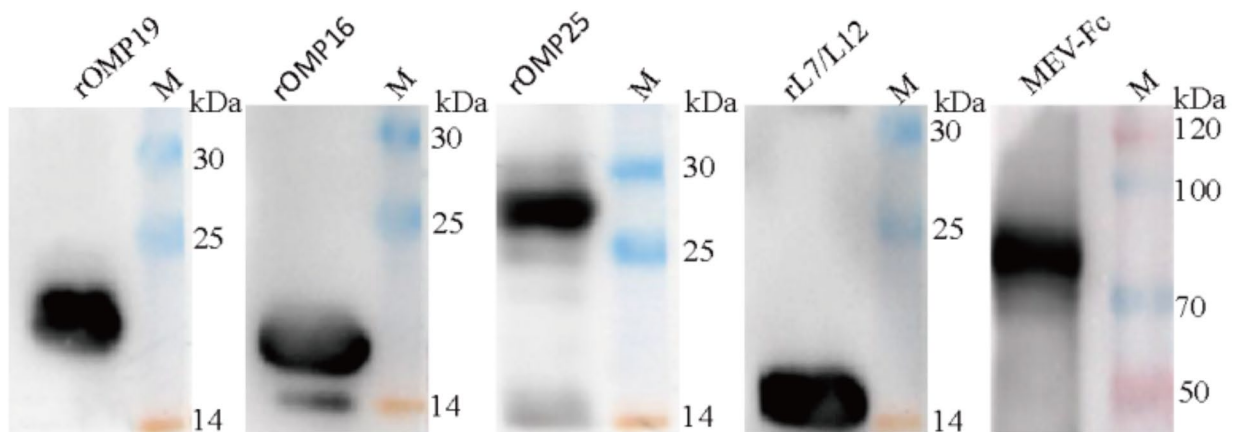
A**B**

Fig. 2 Expression, Purification and Identification of Recombinant Proteins. **(A)** Purification of rOMP19, rOMP16, rOMP25, rL7/L12, and rMEV-Fc proteins using Ni-NTA chromatography. **(B)** Immunoblot analysis of the purified recombinant proteins was performed individually using an anti-His tag antibody

However, the numbers of IFN- γ -secreting T cells in the rMEV-Fc group, S2 group, and rOMP25 group were significantly higher than those in the PBS group (Fig. 4A and B). On the other hand, The immune protection conferred by vaccines requires not only eliciting an immune response but also providing strong immunological memory. To investigate the effect of vaccine administration on lymphocyte proliferation in mice, the CCK-8 method was employed to evaluate lymphocyte proliferation. The

results demonstrated that, in contrast to the control group consisting of unstimulated cells, the lymphocyte proliferation levels in the rMEV-Fc, S2, rOMP16, and rOMP19 groups, all of which were subjected to stimulation, were significantly elevated. (Fig. 4C).

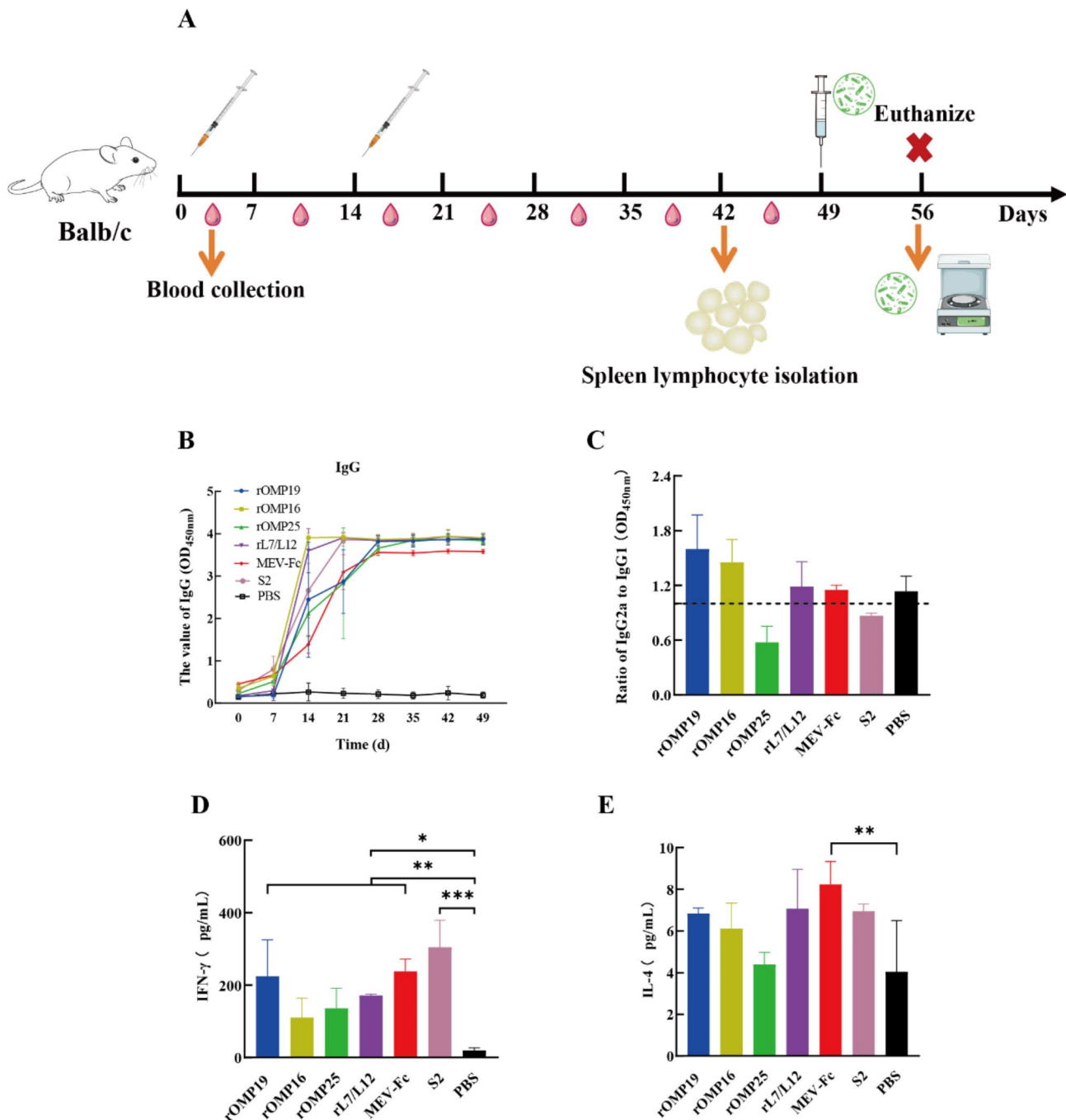


Fig. 3 Immune responses elicited by the candidate vaccine. **(A)** The immunization strategy of mice with MEV-Fc. IgG **(B)**, IgG2a, and IgG1 OD_{450nm} ratios **(C)** were detected using iELISA. Cytokines IFN- γ **(D)** and IL-4 **(E)** levels in serum were measured. Data are presented as mean \pm SD and analyzed using one-way ANOVA. **** p < 0.0001, *** p < 0.001, ** p < 0.01, and * p < 0.05

Flow cytometric analysis of Splenic lymphocytes in immunized mice

To determine the percentages of CD4⁺ and CD8⁺ T cells after immunization, two animals from each group were sacrificed, and splenic lymphocytes were collected. Upon analysis of T cell subtypes, significantly more CD4⁺ and CD8⁺ T cells were observed in the spleen of mice from

the rMEV-Fc group, which were markedly higher than those in the blank control group (Fig. 5). This finding suggests the activation of both humoral and cellular immunity, enabling an effective response to infection or vaccination.

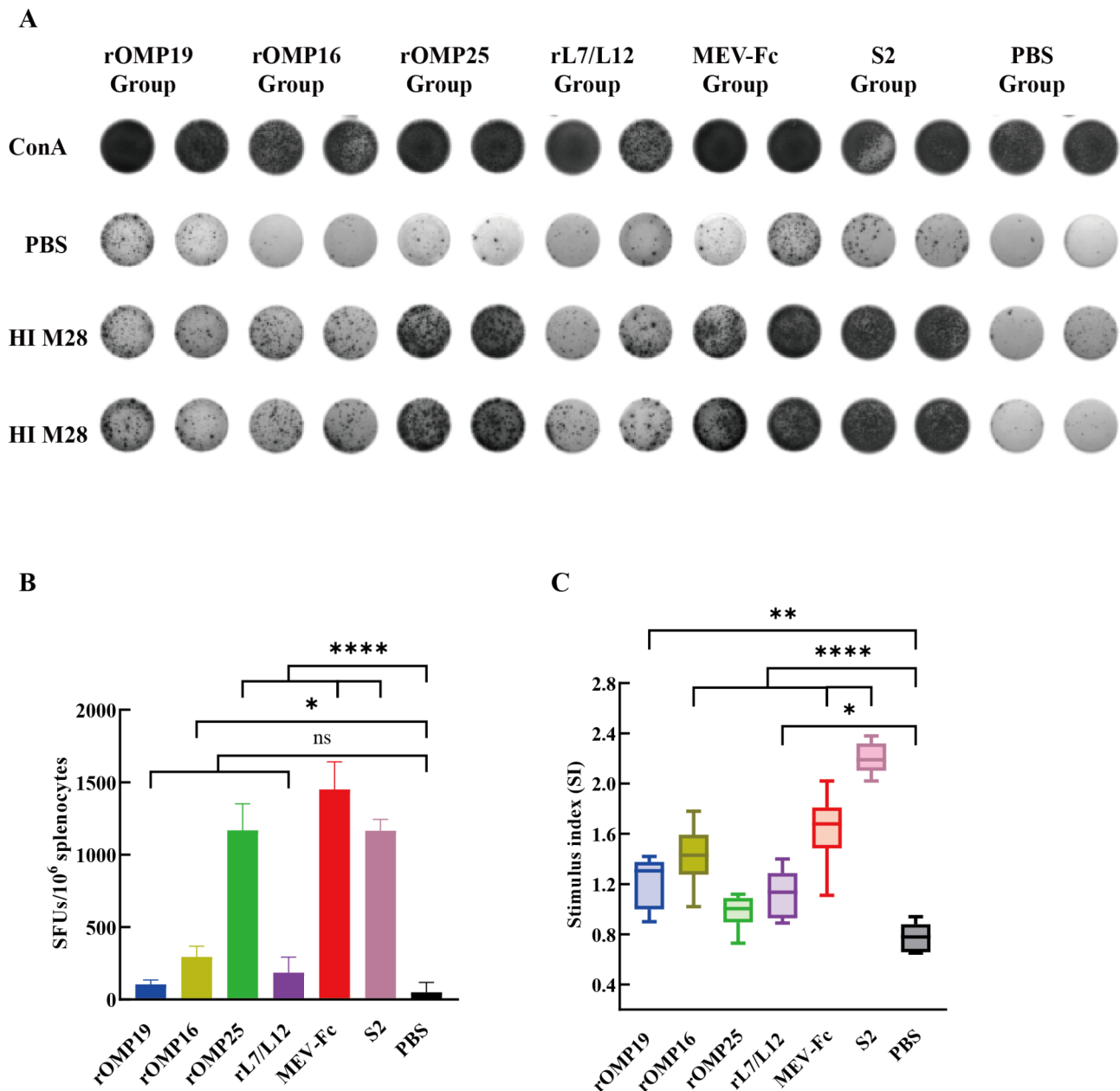


Fig. 4 (A) ELISpot is used to detect the spot-forming units (SFUs) of T cells that secrete IFN in mouse splenic lymphocytes. (B) Quantification of the SFUs of T cells that secrete IFN by ELISpot. (C) CCK-8 assay for the proliferation response of splenic lymphocytes. Data are presented as mean \pm SD and analyzed using one-way ANOVA. **** $p < 0.0001$, *** $p < 0.001$, ** $p < 0.01$, * $p < 0.05$

Vaccines can reduce bacterial load and reduce histological damage in the liver and spleen

We evaluated the protective efficacy of candidate polypeptide vaccines by using a non-lethal *B. melitensis* M28 infection model. The results showed that the S2 group and rMEV-Fc group (protection units of 1.92 and 1.36, respectively) exhibited significant protective effects (Fig. 6A). Considering the strong antibacterial immunity of the rMEV-Fc vaccine against *Brucella*, we further observed the protective effects of rMEV-Fc on the liver and spleen through pathological sections. Moreover,

histological analysis of the spleen and liver of mice infected with *B. melitensis* M28 revealed alleviation of multinucleated giant cell infiltration and proliferation in the spleen, as well as blurring of the red and white pulp structure, and reduction of inflammatory cell infiltration and improvement of the disordered hepatic cord arrangement in the liver (Fig. 6B).

The polypeptide vaccine rMEV-Fc is safe in mice

Given that rMEV-Fc induces an efficient humoral immune response and cellular immune response, and

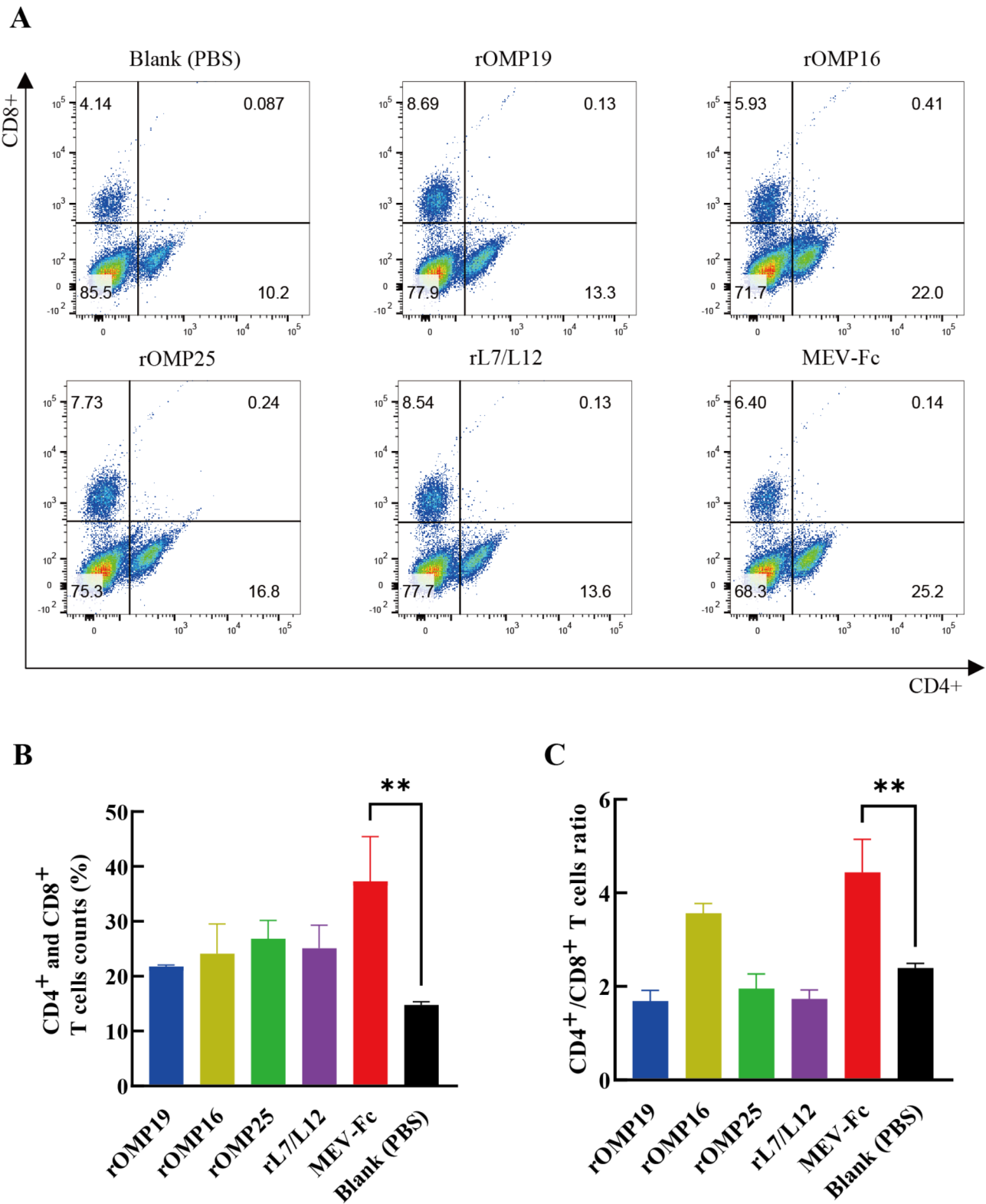
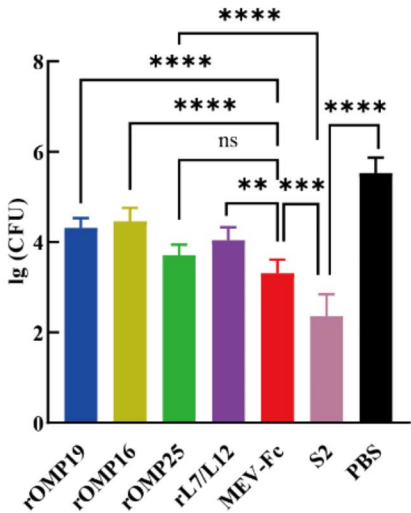


Fig. 5 Flow cytometry analysis: **(A)** Percentage of CD4⁺ and CD8⁺ T cells (*n* = 2). **(B)** Proportion of CD4⁺ and CD8⁺ T cells in splenic lymphocytes. **(C)** Ratio of CD4⁺ to CD8⁺. Data are presented as mean ± SD and analyzed using one-way ANOVA. *****p* < 0.0001, ****p* < 0.001, ***p* < 0.01, and **p* < 0.05

A

Vaccine	Ig(CFU) of M28 in spleen	Unit of protection
rOMP16	4.46 ± 0.29	0.21
rOMP19	4.31 ± 0.22	0.36
rOMP25	3.71 ± 0.22	0.96
rL7/L12	4.04 ± 0.29	0.63
MEV-Fc	3.31 ± 0.31	1.36
S2	2.75 ± 0.49	1.92
PBS	4.67 ± 0.34	-



B

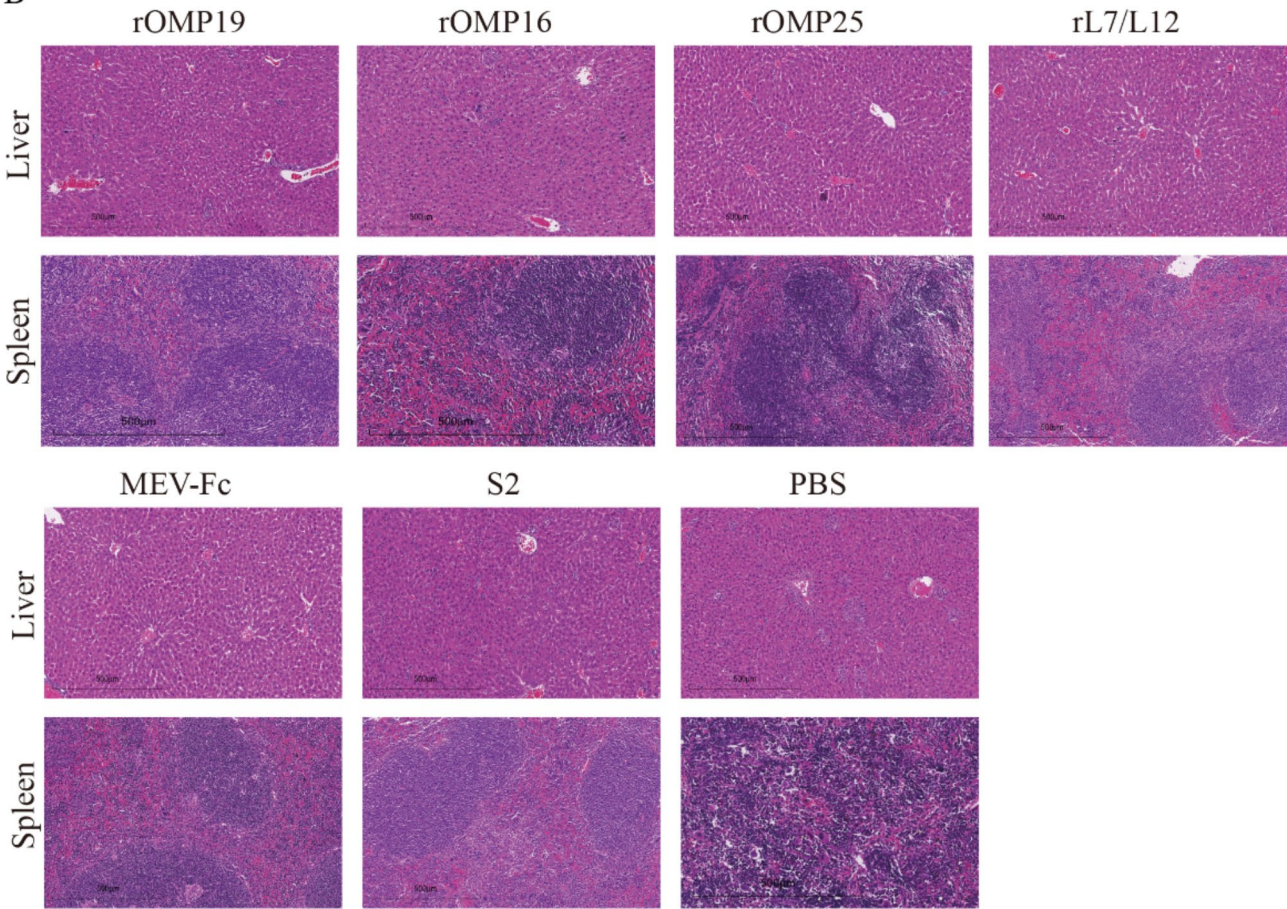


Fig. 6 Evaluation of the Protective Effects of Candidate Vaccines against *B. melitensis* M28 Infection. **(A)** Quantification of bacterial colonization in the spleen of immunized mice six days post-attack. **(B)** Pathological changes in spleens and livers of mice infected with *B. melitensis* M28 on day 6. The scale bar is located at the bottom of the figure (500 μm). Data are presented as mean ± SD and analyzed using one-way ANOVA. *****p* < 0.0001, ****p* < 0.001, ***p* < 0.01, and **p* < 0.05

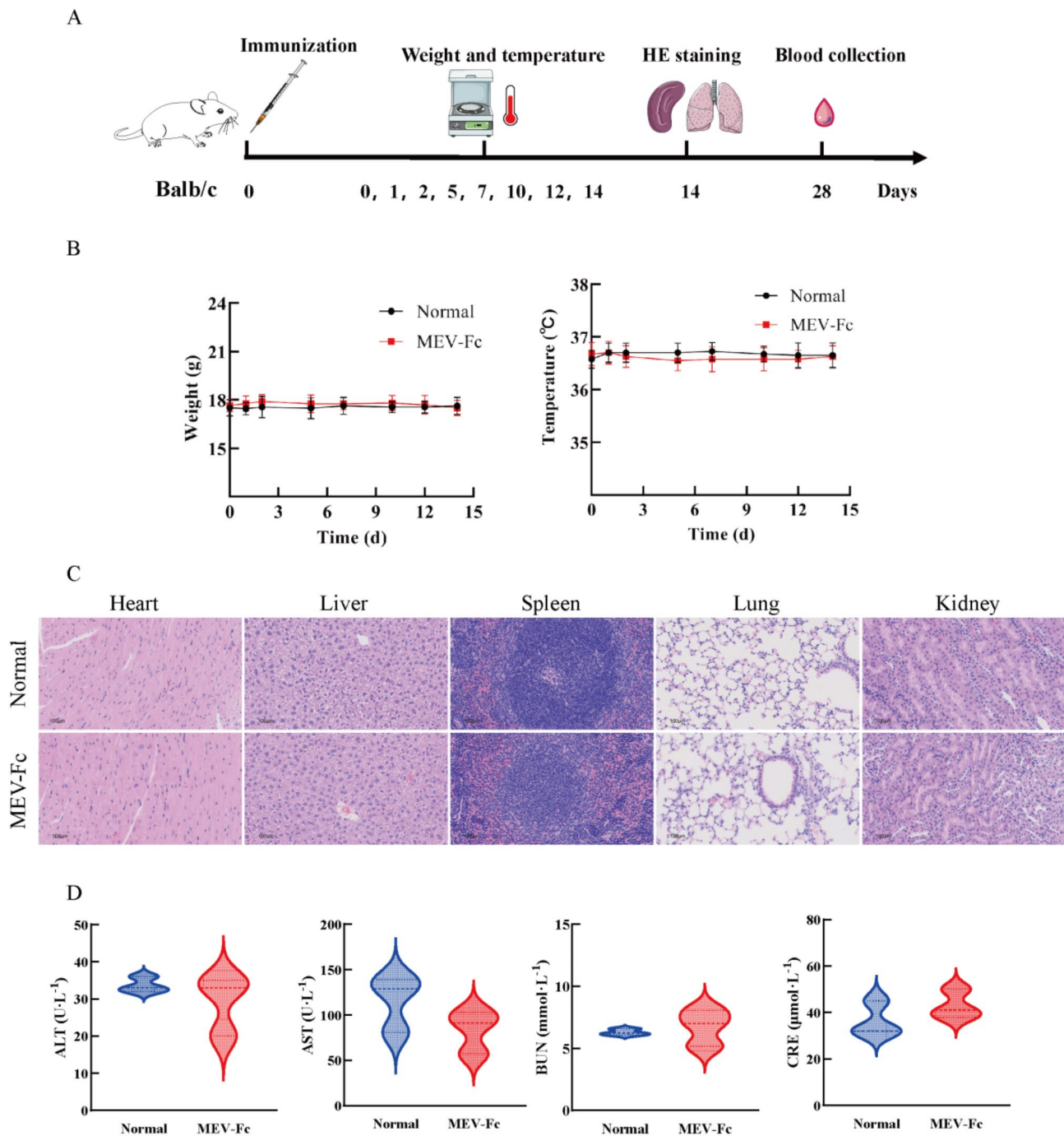


Fig. 7 Safety evaluation of the polypeptide vaccine rMEV-Fc. **(A)** Experimental timeline for the safety evaluation of the peptide vaccine. **(B)** Changes in body weight and rectal temperature of mice treated with MEV-Fc once and normal mice. **(C)** Histological analysis (100 μm) of the heart, liver, spleen, lung, and kidney of treated mice and normal mice on the 14th day after treatment. **(D)** Levels of ALT, ALP, AST, and CRE in the serum of treated mice and normal mice on the 28th day after immunization

may provides immune protection for mice, we further investigated whether rMEV-Fc has any toxic effects in BALB/c mice. Specifically, BALB/c mice were injected with rMEV-Fc (100 μg/100 μL), and then we monitored a series of safety indicators at various time points (Fig. 7A). During the observation period, vaccinated

mice did not exhibit abnormal signs such as weight loss or abnormal body temperature changes (Fig. 7B). On day 14 after administration, histological analyses were performed on organs including the heart, liver, spleen, lungs, and kidneys. As anticipated, no damage or pathological changes were detected in the tissue sections (Fig. 7C).

Additionally, on day 28 post-vaccination, serum biochemical parameters such as ALT, AST, BUN, and CRE were measured, and all biomarkers in both vaccinated and normal (untreated) mice remained within normal ranges (Fig. 7D). These results indicate that the polypeptide vaccine rMEV-Fc is safe.

Discussion

Due to the reemergence of brucellosis worldwide with increasing incidences of human infection, vaccination is considered to be the most effective prevention method [33]. The peptide-based vaccine approach provides an innovative path for vaccine development as it targets the most immunogenic peptide fragments to elicit an immune response, making it an attractive alternative in vaccine research [34]. Yin et al., developed a multi-epitope subunit vaccine from OMP16, OMP2b, OMP31, and BP26 that conferred high levels of protection in mice against *B. melitensis* [35]. The Fc-fusion protein technique is currently one of the most effective strategies for extending the half-life of protein- and peptide-based drugs. Antigen-Fc fusion proteins can specifically target Fc receptors on the surface of antigen-presenting cells, thereby improving their immunogenicity. Fusion of Fc fragments with specific antigens has emerged as a novel vaccination strategy for preventing infectious diseases [36]. Therefore, in our previous study [22], we designed an Fc-fusion multi-epitope vaccine (MEV-Fc) based on the immunodominant epitopes of OMP16, OMP19, L7/L12 and OMP25 to prevent *Brucella* infection.

In this study, we first analyzed the physicochemical properties, secondary structure, and tertiary structure of the candidate vaccine. The results demonstrated that the candidate vaccine exhibited excellent antigenicity, stability, hydrophilicity, solubility, and non-toxicity. Protein regions with native unfolding and α -helices are commonly recognized as typical structural antigens, while β -turns and loosely coiled random structures are more favorable for forming antigenic epitopes [37]. Therefore, candidate vaccines with abundant such structures provide a robust structural foundation for vaccine development. Considering Robetta's outstanding performance in protein tertiary structure prediction, we utilized it to predict the high-quality tertiary structures of the candidate vaccine [38]. Based on the Ramachandran plot, over 98% of residues were located in favorable and allowed regions, indicating the protein structures were accurately predicted. These findings suggest that the candidate vaccine possesses a strong structural basis for vaccine development.

The *E. coli* system offers unique advantages for large-scale production of safe, effective, and cost-efficient subunit vaccines [39]. We employed the *E. coli* expression system to obtain recombinant protein vaccines and

peptide vaccines and evaluated their immunogenicity and protective efficacy in BALB/c mice. For intracellular pathogens, ensuring effective defense mechanisms requires a synergistic interplay of cell-mediated and humoral immune responses [40, 41]. IELISA results showed a significant increase in IgG, IgG1 and IgG2a levels in the sera of mice immunized with all candidate vaccines. In the BALB/c mouse model, IgG1 and IgG2a antibodies serve as indicators of Th2 and Th1 polarization, respectively [42]. The mice immunized in the MEV-Fc group induced a balanced Th1 and Th2 response (the IgG2a/IgG1 ratio was approximately 1.0). Numerous studies claim that the protective immune response against *Brucella* is associated with high-level Th1 and Th2 responses. This implies that candidate vaccines with great potential likely need to simultaneously trigger robust Th1 and Th2 responses to more effectively counter *Brucella* infection [43, 44].

The secretion of IFN- γ activates macrophages, enhances Th1 cell activity, and promotes cellular immune responses, playing a crucial role in *Brucella*-specific cellular immunity [45, 46]. We found that when spleen lymphocytes were stimulated with the candidate vaccine, the MEV-Fc, S2, and rOMP25 groups exhibited significantly higher numbers of IFN- γ -secreting T cells compared to the PBS group. Additionally, IFN- γ secretion levels in mouse sera were detected using iELISA, with rL7/L12, MEV-Fc, and S2 groups showing significantly higher IFN- γ levels than the PBS control group. Interestingly, MEV-Fc and S2 exhibited significantly higher IFN- γ secretion levels in both lymphocyte stimulation and serum compared to the control group, whereas other groups displayed varying trends. One possible explanation is that ELISPOT reflects a localized response, mainly showing the activation of antigen-specific T cells in lymph nodes or the spleen, while serum IFN- γ represents a systemic immune response, which may be influenced by factors such as inflammation levels and reactions of other immune cells [46].

CD4⁺ and CD8⁺ T cells play pivotal roles in the protection offered during *Brucella* infection, with resistance to *Brucella* attributed to their synergistic effects [47]. Several previous studies have shown that both CD4⁺ and CD8⁺ T cells can play important roles in controlling *Brucella* infection [48, 49]. In our results, the CD4⁺/CD8⁺ T-cell ratio and the numbers of CD4⁺ and CD8⁺ T cells in the MEV-Fc group increased significantly. Although the importance of CD4⁺ and CD8⁺ T cells in the immunity against *Brucella* infection has been controversial [50], both of these T-cell populations are likely to be important [51].

Although mice are not the natural hosts of *Brucella*, they are the most commonly used experimental models for studying the in-vivo virulence of *Brucella* [52].

Therefore, in this study, BALB/c model animals were used to evaluate the protective effect of candidate vaccines. We found that the live vaccine (S2) had the highest protective effect against *B. melitensis* M28 infection. This might be because it can effectively infect host cells and generate a variety of endogenous antigens in antigen-presenting cells [53], thereby eliciting a broader and more effective immune response to a real-life infection, which is higher than that of other candidate vaccines. Compared with the OMP16 group, OMP19 group, OMP25 group, and L7/L12 group, the MEV - Fc group had a significant protective effect, which might be attributed to a significant increase in the cellular immune response. These data are exciting because a polypeptide vaccine can provide effective protection in a mouse model of *Brucella*. Subsequently, we will further explore the mechanism by which it protects mice from *Brucella* infection.

Despite the promising nature of the current study, this study also has certain limitations: The synergistic effect between serum IgG and secretory IgA remains unclear. Our lack of knowledge of this mechanism may affect the comprehensive understanding of the immune response and the further optimization of vaccines. The route of immunization plays a crucial role in the immunogenicity of vaccines. In this study, the route of administration and the immunization schedule still need to be optimized. In addition, this study mainly conducted experimental evaluations using BALB/c mouse models. There are certain differences in physiology and immune responses between mouse models and humans, so they cannot fully and accurately reflect the efficacy and safety of vaccines in humans.

Conclusions

MEV-Fc successfully induced robust humoral and cellular immune responses by targeting multiple *Brucella* antigens. This study aimed to develop a polypeptide vaccine against *Brucella*. As a result, a novel peptide vaccine candidate, MEV-Fc, was designed, primarily targeting *Brucella* proteins OMP16, OMP19, L7/L12, and OMP25. By comparing the peptide vaccine containing antigen fragments of all four proteins with single recombinant proteins, we found that the peptide vaccine demonstrated superiority in multiple aspects. The polypeptide vaccine rMEV-Fc significantly stimulated the immune system, eliciting high levels of specific IgG and inducing both Th1 and Th2 responses. Moreover, it provided high protection efficiency in mice following bacterial challenge. Nevertheless, further experiments and clinical trials are needed to comprehensively assess the efficacy of this peptide vaccine under different conditions.

Supplementary Information

The online version contains supplementary material available at <https://doi.org/10.1186/s12934-025-02713-0>.

Supplementary Material 1

Supplementary Material 2

Author contributions

All the authors approved the manuscript for submission. WA, ZY, LC, KZ, HT, YK, LH, FS, LX, ZW, MC, ZC, SJ, MZ, XM, ZJ, YJ and WY contributed to the study design and data interpretation. All the authors contributed to the data analysis and the interpretation of the results. WA, ZY and WY wrote the manuscript and produced all the figures. All authors read and approved the final manuscript.

Funding

This work was supported by the National Natural Science Foundation of China (82160391), the Eighth Division Shihezi Science and Technology Plan Project (2024SF01), the Youth Outstanding Science and Technology Talent Project of Department of Education of Guizhou Province (QJJ [2024] 347), the Shihezi University International Science and Technology Cooperation Promotion Program (No. GJHZ202203), the Tongren Science and Technology Bureau Project (TSKY [2023] 39, TSKY [2024] 6), the Open Project Program of Jiangsu Key Laboratory of Zoonosis (No. R2104), and the Open Project of Key Laboratory of Animal Biopharmaceutical Corps (FM0F2024001).

Data availability

No datasets were generated or analysed during the current study.

Declarations

Ethics approval and consent to participate

All animal experiments were approved by the Bioethics Committee of Shihezi University and conducted in accordance with the Committee's recommendations (A2024-436).

Consent for publication

Not applicable.

Competing interests

The authors declare no competing interests.

Received: 22 January 2025 / Accepted: 5 April 2025

Published online: 15 April 2025

References

1. Pandey A, Cabello A, Akoolo L et al. The case for live attenuated vaccines against the neglected zoonotic diseases brucellosis and bovine tuberculosis [J]. *PLoS Negl Trop Dis*. 2016; 10(8).
2. Franc K A, Krecek R C, Haesler B N et al. Brucellosis remains a neglected disease in the developing world: a call for interdisciplinary action [J]. *BMC Public Health*. 2018; 18.
3. McDermott J, Grace D. Economics of brucellosis impact and control in low-income countries [J]. *Revue Scientifique Et Technique-Office Int Des Epizooties*. 2013;32(1):249–61.
4. Dadar M, Tiwari R, Sharun K, et al. Importance of brucellosis control programs of livestock on the improvement of one health [J]. *Veterinary Q*. 2021;41(1):137–51.
5. Memish Z A, Balkhy HH. Brucellosis and international travel [J]. *J Travel Med*. 2004;11(1):49–55.
6. Gheibi A, Khanahmad H, Kashfi K, et al. Development of new generation of vaccines for *Brucella abortus* [J]. *Heliyon*. 2018;4(12):e01079–01079.
7. Lalsiamthara J, Lee JH. Development and trial of vaccines against *Brucella* [J]. *J Vet Sci*. 2017;18:281–90.
8. Hajissa K, Zakaria R, Suppian R, et al. Epitope-based vaccine as a universal vaccination strategy against *Toxoplasma gondii* infection: A mini-review [J]. *J Adv Veterinary Anim Res*. 2019;6(2):174–82.

9. Geeraedts F, Bungener L, Pool J, et al. Whole inactivated virus influenza vaccine is superior to subunit vaccine in inducing immune responses and secretion of Proinflammatory cytokines by DCs [J]. *Influenza Other Respir Viruses*. 2008;2(2):41–51.
10. Tabynov K, Kydyrbayev Z. Novel influenza virus vectors expressing Brucella L7/L12 or Omp16 proteins in cattle induced a strong T-cell immune response, as well as high protectiveness against *B. abortus* infection [J]. *Vaccine*. 2014;32(18):2034–41.
11. Du Z-Q, Li X, Wang J-Y. Immunogenicity analysis of a novel subunit vaccine candidate Molecule-Recombinant L7/L12 ribosomal protein of *Brucella suis* [J]. *Appl Biochem Biotechnol*. 2016;179(8):1445–55.
12. Pasquevich K A, Estein S M, Samartino C G, et al. Immunization with Recombinant *Brucella* species outer membrane protein Omp16 or Omp19 in adjuvant induces specific CD4+ and CD8+ T cells as well as systemic and oral protection against *Brucella abortus* infection [J]. *Infect Immun*. 2009;77(1):436–45.
13. Gupta S, Mohan S, Somani V K et al. Simultaneous immunization with Omp25 and L7/L12 provides protection against brucellosis in mice [J]. *Pathogens*, 2020, 9(2).
14. Dorneles E M S, Sriranganathan N. Lage A P. Recent advances in *Brucella abortus* vaccines [J]. *Veterinary Research*; 2015.
15. Cloeckaert A, Vizcaino N, Paquet JY, et al. Major outer membrane proteins of *Brucella* spp.: past, present and future [J]. *Vet Microbiol*. 2002;90(1–4):229–47.
16. Carvalho T F, Haddad J P A, Paixao T A et al. Meta-Analysis and advancement of brucellosis vaccinology [J]. *PLoS ONE*, 2016, 11(11).
17. Saadi M, Karkhah A, Nouri HR. Development of a multi-epitope peptide vaccine inducing robust T cell responses against brucellosis using immunoinformatics based approaches [J]. *Infect Genet Evol*. 2017;51:227–34.
18. Onile O S, Musaigwa F, Ayawei N et al. Immunoinformatics studies and design of a potential Multi-Epitope peptide vaccine to combat the fatal visceral leishmaniasis [J]. *Vaccines*, 2022, 10(10).
19. Yusoff S B, Baharum S N B, Omar M S S B et al. Immunoinformatics-guided selection of Immunogenic peptides from betanodavirus induce antigen-specific antibody production in hybrid Grouper, *epinephelus fuscoguttatus* X *epinephelus lanceolatus* [J]. *Aquaculture*, 2024, 579.
20. Ishack S, Lipner SR. Bioinformatics and immunoinformatics to support COVID-19 vaccine development [J]. *J Med Virol*. 2021;93(9):5209–11.
21. Tarrahimofrad H, Zamani J, Hamblin M R, et al. A designed peptide-based vaccine to combat *Brucella melitensis*, *B. suis* and *B. abortus*: Harnessing an epitope mapping and immunoinformatics approach [J]. *Biomedicine & Pharmacotherapy*; 2022. p. 155.
22. Wu A, Wang Y, Ali A, Design of a multi-epitope vaccine against brucellosis fused to IgG-fc by an immunoinformatics approach [J]. *Front Veterinary Sci*, 2023, 10.
23. Gasteiger E, Gattiker A, Hoogland C, et al. ExPASy: the proteomics server for in-depth protein knowledge and analysis [J]. *Nucleic Acids Res*. 2003;31(13):3784–8.
24. Doytchinova I A, Flower D R. VaxiJen: a server for prediction of protective antigens, tumour antigens and subunit vaccines [J]. *BMC Bioinformatics*, 2007, 8.
25. Zhang Q, Wang P, Kim Y, et al. Immune epitope database analysis resource (IEDB-AR) [J]. *Nucleic Acids Res*. 2008;36:W513–8.
26. Sharma N, Naorem L D, Jain S et al. ToxinPred2: an improved method for predicting toxicity of proteins [J]. *Brief Bioinform*, 2022, 23(5).
27. Dodd I B, Egan J B. Improved detection of helix-turn-helix DNA-binding motifs in protein sequences [J]. *Nucleic Acids Res*. 1990;18(17):5019–26.
28. Wiederstein M, Sippl MJ. ProSA-web: interactive web service for the recognition of errors in three-dimensional structures of proteins [J]. *Nucleic Acids Res*. 2007;35:W407–10.
29. Ikai A. Thermostability and aliphatic index of globular proteins [J]. *J BioChem*. 1980;88(6):1895–8.
30. Yang K, Whalen B J, Tirabassi RS, et al. A DNA vaccine prime followed by a liposome-encapsulated protein boost confers enhanced mucosal immune responses and protection [J]. *J Immunol*. 2008;180(9):6159–67.
31. Su Y, Connolly M, Marketon A et al. CryJ-LAMP DNA Vaccines for Japanese Red Cedar Allergy Induce Robust Th1-Type Immune Responses in Murine Model [J]. *Journal of Immunology Research*, 2016, 2016.
32. Hjertner B, Bengtsson T. A novel adjuvant G3 induces both Th1 and Th2 related immune responses in mice after immunization with a trivalent inactivated split-virion influenza vaccine [J]. *Vaccine*. 2018;36(23):3340–4.
33. Olsen S C. Recent developments in livestock and wildlife brucellosis vaccination [J]. *Revue Scientifique Et Technique-Office Int Des Epizooties*. 2013;32(1):207–17.
34. Banerjee A, Santra D, Energetics MAITIS. and IC50 based epitope screening in SARS CoV-2 (COVID 19) Spike protein by immunoinformatic analysis implicating for a suitable vaccine development [J]. *J Translational Med*, 2020, 18(1).
35. Yin D, Li L, Song D, et al. A novel Recombinant multi-epitope protein against *Brucella melitensis* infection [J]. *Immunol Lett*. 2016;175:1–7.
36. Ye L, Zeng R, Bai Y, et al. Efficient mucosal vaccination mediated by the neonatal Fc receptor [J]. *Nat Biotechnol*. 2011;29(2):158–U104.
37. Yu M, Zhu Y, Li Y et al. Design of a Recombinant multivalent epitope vaccine based on SARS-CoV-2 and its variants in immunoinformatics approaches [J]. *Front Immunol*, 2022, 13.
38. Kim D E, Chivian D. Protein structure prediction and analysis using the Robetta server [J]. *Nucleic Acids Res*. 2004;32:W526–31.
39. Incir I, Kaplan O. *Escherichia coli* in the production of biopharmaceuticals [J]. *Biotechnology and Applied Biochemistry*; 2024.
40. Vitry M-A, Mambres D H, De Trez C, et al. Humoral immunity and CD4+Th1 cells are both necessary for a fully protective immune response upon secondary infection with *Brucella melitensis* [J]. *J Immunol*. 2014;192(8):3740–52.
41. Peddayalachagiri B V Pauls. Recombinant outer membrane protein 25c from *Brucella abortus* induces Th1 and Th2 mediated protection against *Brucella abortus* infection in mouse model [J]. *Mol Immunol*. 2018;99:9–18.
42. Firacative C, Gressler A E, Schubert K et al. Identification of T helper (Th)1-and Th2-associated antigens of *Cryptococcus neoformans* in a murine model of pulmonary infection [J]. *Sci Rep*, 2018, 8.
43. Ghasemi A, Jeddi-Tehrani M, Mautner J, et al. Simultaneous immunization of mice with Omp31 and TF provides protection against *Brucella melitensis* infection [J]. *Vaccine*. 2015;33(42):5532–8.
44. Ghasemi A, Jeddi-Tehrani M, Mautner J, et al. Immunization of mice with a novel Recombinant molecular chaperon confers protection against *Brucella melitensis* infection [J]. *Vaccine*. 2014;32(49):6659–66.
45. Xu L, Hao F, Wang J et al. Th1 and Th17 mucosal immune responses elicited by nasally inoculation in mice with virulence factors of *Mycoplasma hyopneumoniae* [J]. *Microb Pathog*, 2022, 172.
46. Mezouar S, Mege J-L. Changing the paradigm of IFN- γ at the interface between innate and adaptive immunity: Macrophage-derived IFN- γ [J]. *J Leukoc Biol*. 2020;108(1):419–26.
47. Huynh Tan H, Tran Xuan Ngoc H, Reyes A W B et al. Interleukin 6 promotes *Brucella abortus* clearance by controlling bactericidal activity of macrophages and CD8+T cell differentiation [J]. *Infect Immun*, 2019, 87(11).
48. He YQ, Vemulapalli R, Zeytun A, et al. Induction of specific cytotoxic lymphocytes in mice vaccinated with *Brucella abortus* RB51 [J]. *Infect Immun*. 2001;69(9):5502–8.
49. Muñoz-Montesino C, Andrews E, Rivers R, et al. Intraspinal delivery of a DNA vaccine coding for superoxide dismutase (SOD) of *Brucella abortus* induces SOD-specific CD4+ and CD8+ < T cells [J]. *Infect Immun*. 2004;72(4):2081–7.
50. Yingst S, Hoover D L. T cell immunity to brucellosis [J]. *Crit Rev Microbiol*. 2003;29(4):313–31.
51. Araya L N, Elzer P H, Rowe G E et al. Temporal development of protective cell-mediated and humoral immunity in BALB/c mice infected with *Brucella abortus* [J]. *Journal of immunology (Baltimore, Md: 1950)*, 1989;143(10):3330–3337.
52. Silva T M A, Costa E A, Paixao T A, et al. Laboratory animal models for brucellosis research [J]. *J Biomed Biotechnol*. 2011;2011:518323–518323.
53. Luo D, Bing N, Li P, et al. Protective immunity elicited by a divalent DNA vaccine encoding both the L7/L12 and Omp16 genes of *Brucella abortus* in BALB/c mice [J]. *Infect Immun*. 2006;74(5):2734–41.

Publisher's note

Springer Nature remains neutral with regard to jurisdictional claims in published maps and institutional affiliations.